

RESEARCH ARTICLE

Genetic Algorithm-Based Commutation Angle Control for Torque Ripple Mitigation in Switched Reluctance Motor Drives

RENATA REZENDE C. REIS¹, MARCIO L. MAGRI KIMPARA², (Member, IEEE),
LUIGI GALOTTO JR.¹, (Member, IEEE),
AND JOÃO ONOFRE PEREIRA PINTO², (Senior Member, IEEE)

¹Faculty of Engineering, Architecture and Urbanism and Geography, Federal University of Mato Grosso do Sul, Campo Grande 79070-900, Brazil

²Oak Ridge National Laboratory, Oak Ridge, TN 37830, USA

Corresponding author: Renata Rezende C. Reis (renatarezendereis@gmail.com)

This work was supported in part by the Brazilian National Council for Scientific and Technological Development (CNPq) under Grant 429543/2016-6, and in part by the Coordenação de Aperfeiçoamento de Pessoal de Nível Superior—Brazil (CAPES)—Finance Code 001.

ABSTRACT This work addresses the application of the Genetic Algorithm (GA) technique to optimize the commutation angles of a 2 kW 8/6 switched reluctance machine (SRM). The primary goal is to reduce the well-known drawback of SRMs: the torque ripple. Firstly, the machine was modeled in Matlab/Simulink® using lookup tables obtained via finite element method (FEM) simulations. Subsequently, the model was used to perform the GA routine aiming to find the optimal phase commutation angles that minimize the torque ripple factor. Notably, the torque performance of the SRM was significantly affected by the commutation angles during the search for the optimal solution. Afterwards, the GA results for four different operation points were verified experimentally through a developed drive platform with digital signal processor-based (DSP) control and an asymmetric bridge converter. As showed by the experiments, the proposed approach was suitable to reduce the torque ripple by more than 50% for one of the evaluated operating points. Furthermore, it was confirmed that the torque ripple mitigation led to acoustic noise improvement.

INDEX TERMS Switched reluctance motor, genetic algorithm, optimization, torque ripple.

I. INTRODUCTION

The research on Switched Reluctance Motors (SRM) has been recently intensified with such a motor being designed and tested for several applications, including industrial, domestic, space, and mobility [1]. The characteristics of the SRMs such as robustness, high power density, wide speed range, low cost, and high efficiency, stands-out when compared to their counterparts, making them attractive candidates for certain applications. Despite the advantages of the SRM, the inherent torque pulsation and high audible noise can be considered limiting factors for the widespread use of this type of motor [2], [3]. Therefore, to take the most advantage of

the SRM features in general applications and to enable its use in cases where the load is sensitive to torque pulsation, the SRM design or its drive system, or both, must undergo an optimization process [4].

The optimization can be accomplished either by modifying the machine geometry to guarantee that its structure contributes to the expected performance, or by optimizing the motor drive by means of control techniques to comply with the requirements imposed by the load [5]. Albeit there are several SRM design insights in the literature, this approach is suitable for early design stages and becomes more complex as different aspects are added to the package of constraints, requiring multiphysics and multi-objective optimization [6], [7]. Thus, optimization via advanced control to improve the SRM performance becomes desirable

The associate editor coordinating the review of this manuscript and approving it for publication was Christian Pilato¹.

in some cases, especially when a target machine is already built.

The torque ripple in SRMs has its origin in the sequential phase excitation pattern and the non-linear inductance variation concerning the rotor position. Hence, many techniques have been reported to decrease torque ripple through direct and indirect methods [8], [9], [10].

In addition, authors in [11] used Particle Swarm Optimization (PSO) to define the appropriate switching angles. Although the results are suitable, the PSO does not present evolutionary operators, increasing the number of iterations to obtain a satisfactory result. In [12], a modified Hybrid Whale Optimization Algorithm (mWOA) is compared with Whale Optimization Algorithm (WOA) for control of speed along with ripple reduction in output torque of a 75 kW SRM drive. Another metaheuristic technique that can be applied to solve problems concerning electric machines is the Genetic Algorithm (GA). Accordingly, in [13], the GA was used to compare different designs of a 24/16 SRM. In this case, the best-performing design had its optimal angles defined from a multi-objective optimization to maximize the average torque and minimize the torque ripple throughout the operating speed range. In more recent works, such as [14], GA is used to seek the optimal value of the weight parameter related to the excitation current, thus printing a small ripple within a routine that includes the Torque Sharing Function (TSF) technique. Similarly, GA was used in [15] to achieve an improved TSF with lower current tracking error for torque ripple reduction in SRMs. Targeting to minimize the torque ripple, authors in [16] developed specific optimization objectives for conduction angle control during generating mode.

The present study comprehends the optimization of the phase turn-on and turn-off angles of a 2 kW 8/6 SRM based on the application of the Genetic Algorithm, aiming to smooth the torque profile for the machine operating below the base speed. The main contribution of this work is the development of a methodology that can be applied, with few adjustments, to any SRM demonstrating the potential for improving the performance of this type of motor, if a proper drive system is used. The adopted approach is easily deployed and combines the use of the Finite Element Method (FEM) to obtain the electromagnetic signature of the target motor with acceptable accuracy, and the GA as the optimization search technique. The effectiveness of the proposed method was evaluated through simulation and experimental results, and it was observed an improvement up to 50% for one of the operation points.

II. TORQUE RIPPLE ORIGIN AND EFFECT OF THE COMMUTATION ANGLES

The switched reluctance motor features a doubly salient structure with a particular rotor, free of windings and permanent magnets. The working principle of the SRM is established on the alignment tendency between the rotor and stator poles when the concentrated stator phase winding is excited. Accordingly, the continuous movement in motor mode occurs

with the sequential excitation of the stator phases, leading the generated torque to be the sum of the torque produced by individual phases. Nonetheless, this switched operation leads to a torque droop that occurs in the commutation region between two phases as a result of two factors: i) if the upcoming phase is not turned on in a proper instant, the torque produced by the respective phase will take some time to arise, affecting the overall torque profile; ii) the generated torque T is proportional to the slope of the inductance L (1) [4], which presents a non-linear relationship with respect to the rotor position θ , thus, the torque value decreases as the poles approach complete alignment (point of constant inductance). These two factors combined give rise to the torque ripple T_{ripple} , calculated by (2), where T_{max} , T_{min} , and T_{avg} stand for maximum, minimum and average torque, respectively.

To minimize the torque pulsation by means of control strategies, one method is to simultaneously excite two adjacent phases [17]. This overlapped operation has a great impact on torque generation; however, it is not always beneficial, i.e., it can adversely affect the average torque. Therefore, defining the dwell angle for each phase (turn-on and turn-off angles) becomes an optimization problem. Furthermore, the optimal angles may vary from one operation point to another.

$$T = \frac{1}{2} i^2 \frac{dL(\theta, i)}{dt} \quad (1)$$

$$T_{ripple} = \frac{T_{max} - T_{min}}{T_{avg}} \times 100\% \quad (2)$$

Figure 1(a) presents three theoretical excitation profiles that show the effects of commutation angles (θ) on torque generation in Fig. 1(b) and Fig. 1(c). As depicted, profile 1 comprehends a short excitation period ($\theta_1 - \theta_3$), which despite presenting a lower magnitude for both RMS current and ohmic losses, gives rise to a low-quality overall torque once its average value is reduced and high torque pulsation is noticed. The reason is the large interval until the next phase gets excited. In profiles 2 and 3, the phase conduction period is longer, improving the quality of the generated torque. Another visible effect in the last two profiles is the generation of negative torque, given the delay in turning off the excitation of outgoing phase. This effect is caused by the presence of electric current during the negative derivative of the phase inductance that takes place after the complete alignment of the poles. It is noteworthy that some negative phase torque can be tolerated for the benefit of the total torque generated on the shaft, however, the amount of negative torque must be carefully controlled through the turn-off angle.

The power electronics-based drive controls the motor phase excitation, and the asymmetric bridge converter is a commonly used topology due to its flexibility. As shown in Figure 2, this converter presents two switches and two diodes per phase and allow independent control of all phases. Besides controlling the commutation angles, the amplitude of the electric current may or may not be controlled, depending on the speed of the SRM. At low speeds, the slope of the electric current is steep, which implies the need to limit its

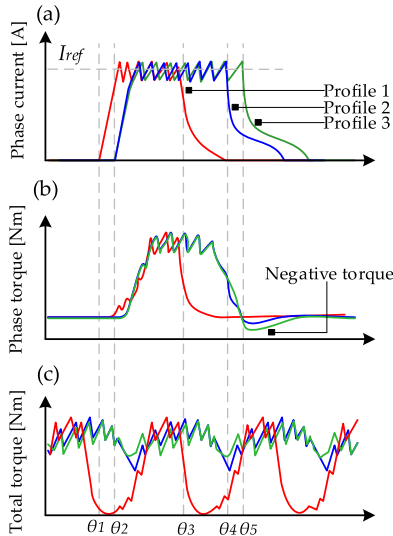


FIGURE 1. Effects of angle changing in SRM current torque [18].

amplitude, using, for example, the hysteresis current control. Conversely, during motor operation at high speeds, the back-emf becomes dominant and helps to prevent the electric current from reaching high values, as shown in Figure 3. In this work, the methodology is focused on operating points below the nominal speed.

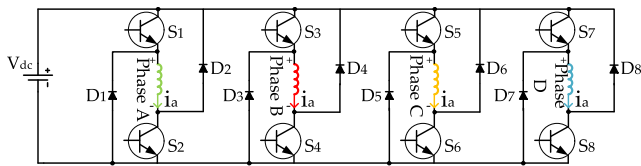


FIGURE 2. Asymmetric bridge converter.

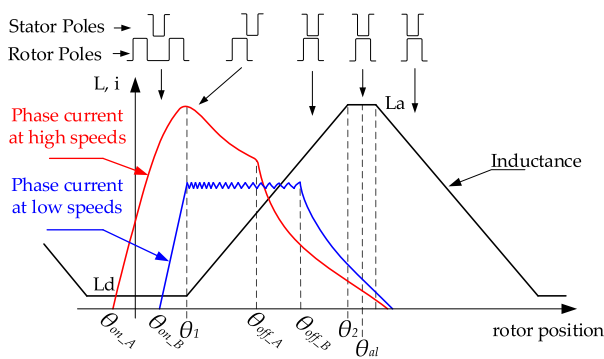


FIGURE 3. Current shape patterns.

III. MODELING AND OPTIMIZATION PROCESS

As previously mentioned, the phase commutation angles affect the average output torque, efficiency, and torque ripple factor of the SRM. Searching for the optimal values for these control parameters can be time-consuming if done exhaustively or lead to non-optimum values if done by trial and error. Therefore, optimizing techniques such as GA can be

employed to speed up the process. As shown in Figure 4, θ_{on} and θ_{off} are the angles at which each phase is energized and de-energized, respectively. The operating point is defined by the speed (ω_{ref}) and the reference electrical current (I_{ref}).

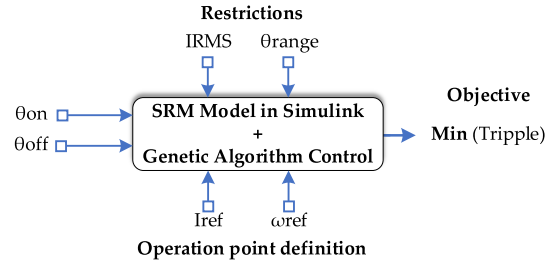


FIGURE 4. Optimization problem definition.

The maximum allowed RMS electrical current (I_{RMS}) and the angle search region (θ_{range}) are constraints to the optimization process, which has as objective the minimization of torque ripple (T_{ripple}). For each desired operating point, values of θ_{on} and θ_{off} are evaluated using a model in Matlab/Simulink. From the results, the GA operators update these angles toward optimal values.

A. FEM RESULTS AND SIMULINK MODEL

The model implemented in Simulink incorporates both the torque and flux look-up tables to represent the SRM under study, as well as the analytics equations that describe the drive model, which makes it computationally less expensive, a desirable feature for an iterative search algorithm. The torque and flux data were obtained through the FEMM software covering different values of current and rotor position. These profiles are commonly used to model the SRM since the high nonlinearity of the parameters prevents an accurate model from being developed based only on linear equations. A picture and specifications of the prototype used in this study are shown in Figure 5 and Table 1, respectively. The results obtained for flux and torque profiles are shown in Figure 6 (a) and (b), respectively.

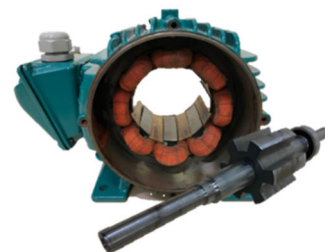


FIGURE 5. 2kW SRM under study.

B. FIRING ANGLES OPTIMIZATION VIA GA

It is clear from the SRM operating profiles that, to maximize the torque performance, θ_{on} must be allocated close to the minimum inductance so the electric current reaches an amplitude that takes advantage of the beginning of the

TABLE 1. SRM parameters.

Symbol	Quantity	Value
P	Power Level	2 kW
n	Base speed	3,500 rpm
V	Voltage	180 V
I_{rms}	RMS current	6 A
-	Lamination material	E185
g	Airgap	0.3mm
D_s	Stator outer diameter	160 mm
D_r	Rotor outer diameter	90.5mm
L	Stack length	81 mm

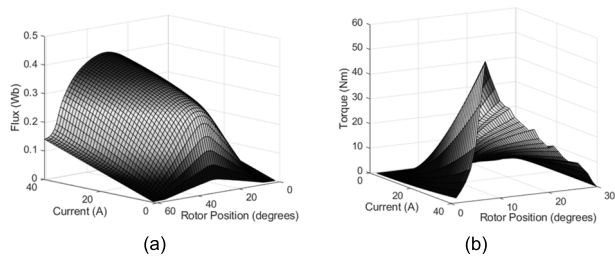


FIGURE 6. FEM profiles as function of current and rotor position. (a) Flux. (b) Static torque.

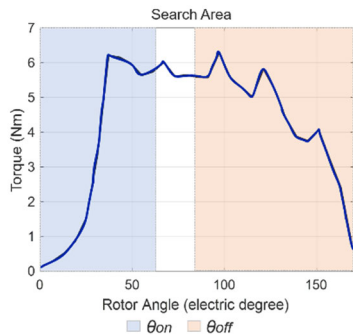


FIGURE 7. GA Search region for a given phase current.

positive derivative of the inductance for torque generation. θ_{off} , on the other hand, must be near the maximum inductance point, so the electric current has enough time to decay without causing an excessive negative torque generation.

The objective function (3) addressed in this paper is to minimize the torque oscillation (T_{ripple}) for a given operating point, which is defined by the speed (ω_{ref}) and the maximum RMS electric current (I_{rms}). The search region is established in a range of possible commutation angle values, as shown in Fig. 7, θ_{upp} and θ_{low} are the upper and lower limits of the search region.

$$\mathbb{F} = \min(T_{ripple}), \begin{cases} I_{rms} \leq \max(I_{rms}) \\ \theta_{on_low} \leq \theta_{on} \leq \theta_{on_upp} \\ \theta_{off_low} \leq \theta_{off} \leq \theta_{off_upp} \\ \omega_{ref} = \omega \end{cases} \quad (3)$$

The optimization process was developed using a co-simulation based on a Simulink SRM customized model and

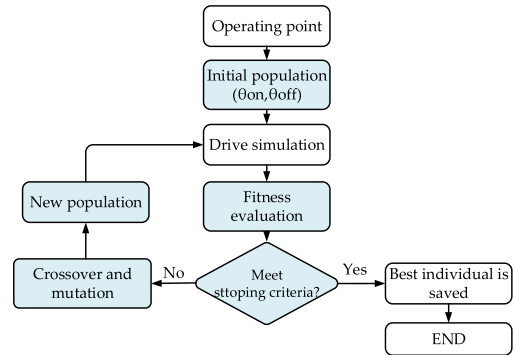


FIGURE 8. Optimization process flowchart.

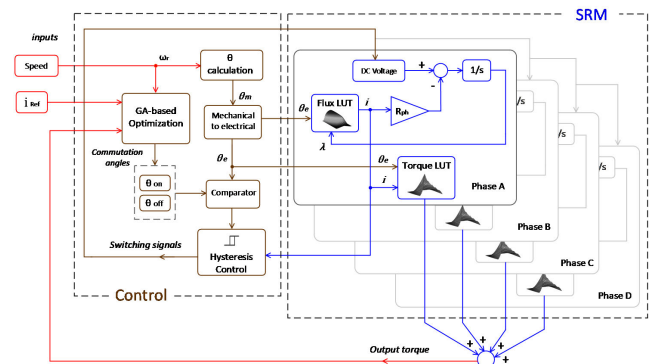


FIGURE 9. SRM model coupled with GA in Matlab/Simulink.

the Global Optimization Toolbox. As per the GA optimization process, a population of angles is created, and the values are applied to the SRM model generating the respective torque responses. These results are evaluated calculating the fitness function from which a new generation of individuals (pair of angles) is obtained through the algorithm operators. In this study, the GA characteristics were defined as follows: Population size equal to 5 individuals, max number of generations equal to 10, selection method: roulette, Fitness function: torque ripple (equation 2), and search region: θ_{on} from 0 to 60 degrees and θ_{off} from 90 to 180 degrees, as shown in Figure 7. Figure 8 presents the flowchart of the implemented method. Given that at each iteration it is necessary to evaluate the fitness function of each individual, the population size and the maximum number of generations were defined based on preliminary tests, selecting values that returned good convergence with low computational cost. To confirm that a larger population was not required to solve this problem, the angles generated in each iteration had their values increased by an increment ($\pm\Delta\theta$), resulting in no significant variations that justify a greater number of individuals to improve the coverage of the search region. Figure 9 illustrates a block diagram of the model implemented in Simulink.

IV. SIMULATION RESULTS

The steps shown in the flowchart of Fig. 8 were performed for 4 defined operating points, i.e., 160, 200, 360 and 600 rpm.

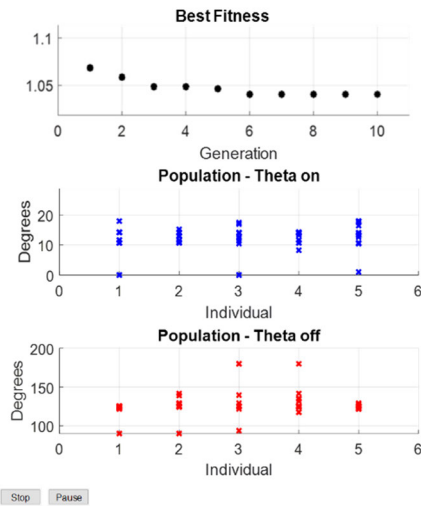


FIGURE 10. GA convergence for a given speed.

TABLE 2. Optimization results.

Speed	Optimized θ_{on}	Optimized θ_{off}
160 rpm	15	120
200 rpm	9	117
360 rpm	6	98
600 rpm	7.5	104

Figure 10 shows the convergence process and the evolution of the individuals (θ_{on} and θ_{off}) during the search for optimal angles when the speed was 160 rpm. One can notice that as the evolutionary process goes, the individuals (1 to 5) get concentrated around 15° electrical degrees for θ_{on} and around 120° for θ_{off} , indicating that the combination of those two angles is to be used in order to operate the SRM with minimal torque ripple. Table 2 presents the best results obtained via GA for all the operating points tested. The algorithm was performed several times to avoid local minima and the total execution time averages 130 seconds on an Intel i5 3317U @1.7GHz processor.

To verify the improvement achieved, the simulation results of conventional and optimized switching angles were compared. According to [19], conventional switching refers to maintaining the phase current during 1 torque production cycle, which in the case of an 8/6 machine represents 15 mechanical degrees. Figure 11 (a) illustrates the comparison between the torque generated with the non-optimized commutation angles and those obtained by the optimization process, which lead to some overlapping between phase currents. For that specific case, a 48% reduction in the ripple factor was observed. The comparative results for the other points shown in Table 2 are illustrated in Figures 11 (b), (c), and (d). One can observe that the proposed optimization successfully reduced the torque oscillation for all the tested conditions, reaching up to more than 50% when operating at 200 rpm.

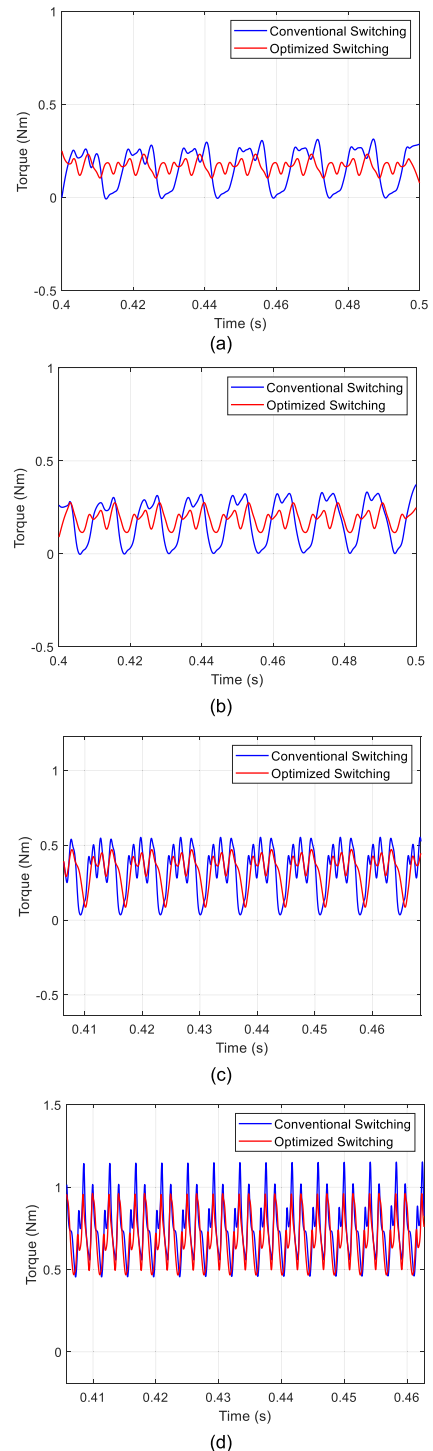


FIGURE 11. Simulation results comparing optimized angles and conventional angles. (a) @160 rpm with 48% of torque ripple reduction (b) @200 rpm with 53% of torque ripple reduction. (c) @360 rpm with 22% of torque ripple reduction. (d) @600 rpm with 23% of torque ripple reduction.

V. EXPERIMENTAL RESULTS

The optimal angles found with the GA method were assessed experimentally for the target SRM coupled with a DC machine acting as load. To measure the instantaneous torque, a torque meter was connected in between the two machines.

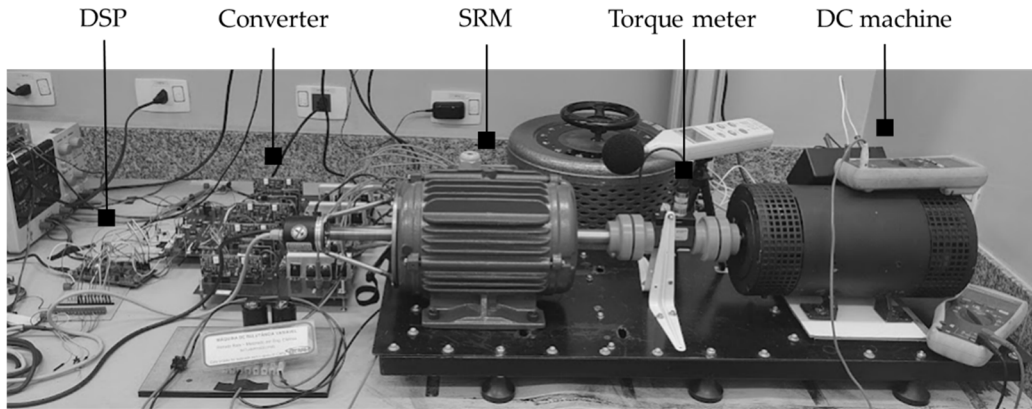


FIGURE 12. Experimental setup.

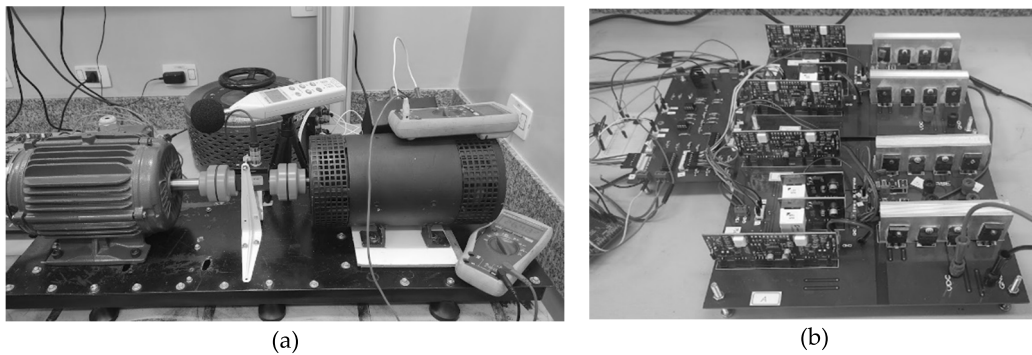


FIGURE 13. Details of the experimental setup. (a) Load connection (torque meter in between). (b) Converter and control boards.

All the experimental tests were conducted in the setup shown in Fig. 12. The load connection and the converter built are shown in Fig. 13 (a) and (b). The hysteresis current control was implemented on a F28379-D DSP with the optimal firing angles stored in a lookup table. To obtain the rotor position and current measurements, a 10 bits absolute encoder EPM50S8-1013-B-S-24 and current sensors model ACS 712 were used. The 4-phase asymmetric bridge converter was designed and implemented for this application using gate drives model DRO100D25.

During the tests, the speed was kept constant based on the reference current, adjusted right after the firing angles were commanded. Furthermore, the resistive load connected to the DC generator remained unchanged, making the load torque dependent on the speed. Due to the resistive load power ratings, the tests were conducted at limited power. Figure 13 presents the achieved results for different speeds.

The experimental results confirmed that the overall torque profile was improved by reducing the ripple while maintaining the average torque.

Moreover, by comparing the current profiles one can notice that such torque improvement was obtained after shifting both commutation angles (on and off), compared to the conventional ones, and that they are different for each speed.

The RMS value of the electrical current required when operating under optimized angles is smaller than that required by the conventional excitation. The analysis of the RMS electrical current is quite relevant to account for the losses. The effect of reducing the RMS current can be understood using (4). It is noted that the value of the electric current depends on the switching angles, which define the conduction period.

$$I_{RMS} = \sqrt{\frac{1}{\theta_{off} - \theta_{on}} \int_{\theta_{on}}^{\theta_{off}} I(\theta)^2 d\theta} \quad (4)$$

Thus, each angle setting will generate a different RMS electrical current profile. This effect occurs due to the different regions of torque generation in SRM, which are dictated by the non-linearity present in the SRM. For example, if the phase is excited in a region capable of generating high torque, an electric current of smaller amplitude is expected. Table 3 presents the summary of average torque and RMS current for each case tested.

The presence of high levels of audible noise is another characteristic of SRMs that ends up hindering its use in some applications. Accordingly, a decibel meter was placed near the drive system and the sound level was measured during the tests. The graphics illustrated in Figure 15 show

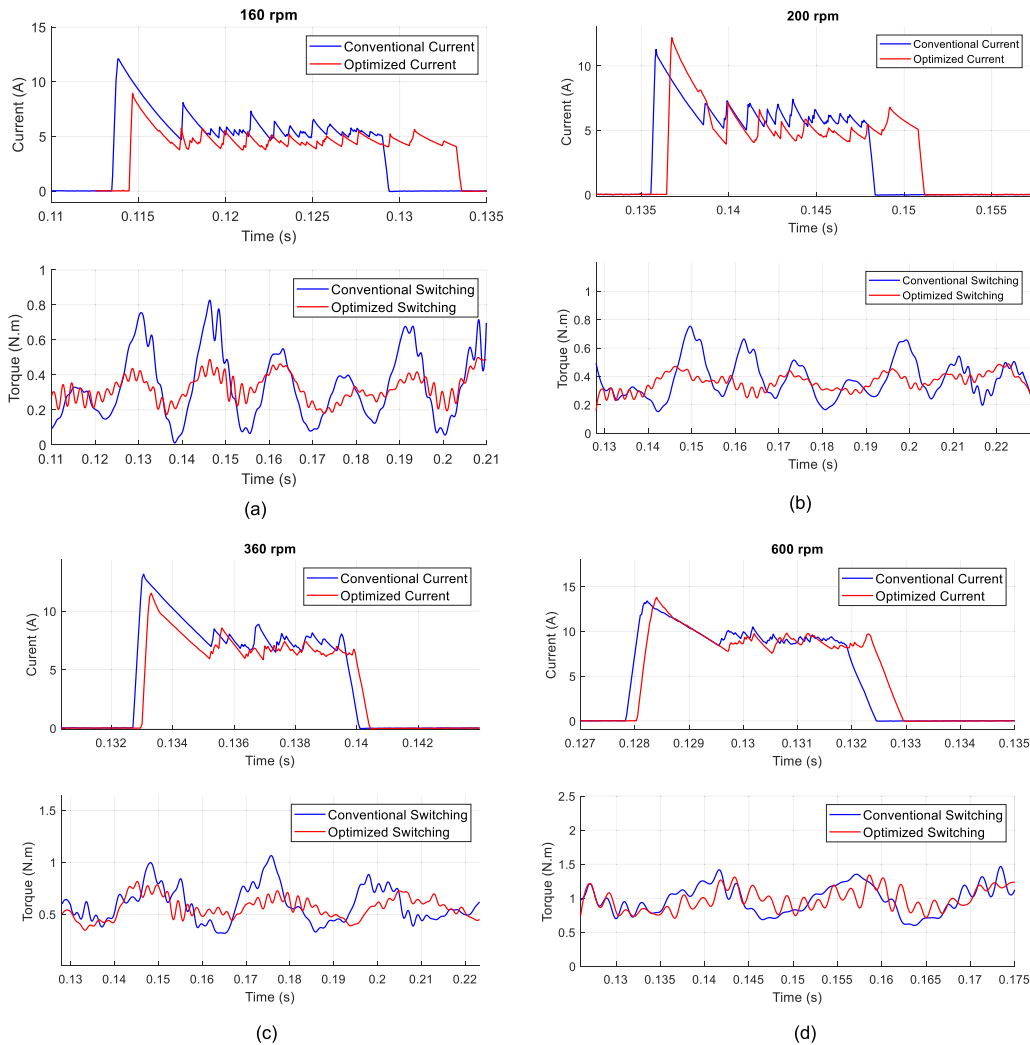


FIGURE 14. Phase current and torque measured experimentally. (a) @160 rpm. (b) @200 rpm. (c) @360 rpm. (d) @600 rpm.

TABLE 3. Comparative results.

Speed	Parameter	Conventional	Optimized
160 rpm	T_{avg}	0.167 Nm	0.167 Nm
	I_{RMS}	3.44 A	3.20 A
200 rpm	T_{avg}	0.18 Nm	0.17 Nm
	I_{RMS}	3.33 A	3.16 A
360 rpm	T_{avg}	0.334 Nm	0.331 Nm
	I_{RMS}	4.38 A	4.02 A
600 rpm	T_{avg}	0.75 Nm	0.71 Nm
	I_{RMS}	5.21 A	4.98 A

the results before and after optimizing the commutation angles. Although the main cause of acoustic noise in SRMs is the vibration due to stator deformation caused by radial forces, the results showed some improvement concerning noise, after mitigating the torque ripple by controlling the angles, similarly to the results in [20]. This can be explained observing that the optimized commutation angles give rise

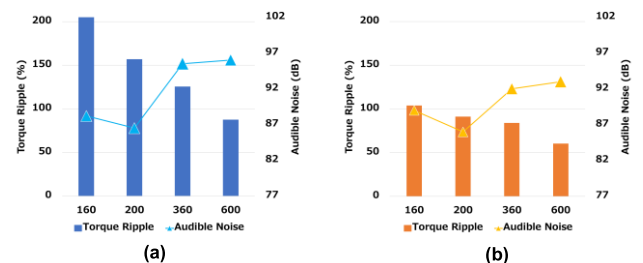


FIGURE 15. Audible noise vs. Torque ripple. (a) Conventional drive. (b) Optimized drive.

to phase-overlapped excitation. In addition, improving the torque pulsation on the shaft helps to prevent mechanical vibration.

Analyzing the collected data, it was also possible to notice the tendency of higher acoustic noise with the increase of speed, which can have electrical origins (higher switching frequency given the greater speed) and aerodynamics, given the movement of the air inside the SRM housing.

Aerodynamic noise can be subdivided into categories, such as exhaust noise, intake noise, cavities, and rotating pressure fields. All types are directly linked to the movement of air through the interior of the machine structure. In this case, the emitted frequency is a function of the air velocity, since it is generated by the rotor poles given the peculiar geometry of the rotating part, which ends up working as a blade fan [21]. Despite these factors, the measured audible noise was reduced by 3.5% for the highest tested speed.

VI. CONCLUSION

This paper presented a comprehensive application of Genetic Algorithms as an optimization method for improving the performance of an 8/6 SRM focused on reducing torque ripple. The approach offers a straightforward yet effective means of determining commutation angles that result in lower torque ripple while maintaining average torque levels.

Simulation and experimental analysis have demonstrated the effectiveness of GA-based optimization across four different operating points, outperforming the conventional excitation. The most significant result was observed at low speed, given the setup limitations. In this case, the reduction of 57.9% in torque ripple represents a considerable improvement, in addition to the implications for the overall efficiency of the drive system. By operating under these optimized angles, the SRM required less RMS electrical current, resulting in lower power losses. Therefore, this optimization strategy presents an opportunity for energy savings and enhanced system performance in real-world applications. Moreover, it was noted that the benefits of enhancing the torque profile extend to a reduction in acoustic noise emissions, addressing another key shortcoming associated with SRMs, and contributing to a more attractive option for noise-sensitive applications.

The achieved reduction in torque ripple, accompanied by lower RMS electrical currents and reduced acoustic noise emissions, points to an overall enhancement in the motor's efficiency, reliability, and acoustic performance. As indicated by the results, the optimal commutation angles vary depending on the desired speed. To extend these results across the entire speed range, a future investigation involves implementing a neural network-based control system, allowing for the generalization and estimation of the optimal angles for different speeds. This approach may enhance the motor's performance and efficiency across all operational ranges.

ACKNOWLEDGMENT

The authors would like to thank the Brazilian Research Agency CAPES and the Graduate Program of Electrical Engineering with the Federal University of Mato Grosso do Sul.

REFERENCES

- [1] A. Spampinato, G. Forte, G. Scelba, and G. De Donato, "A cost-effective switched reluctance motor drive for vacuum cleaners," in *Proc. Int. Symp. Power Electron., Electr. Drives, Autom. Motion (SPEEDAM)*, Sorrento, Italy, Jun. 2020.
- [2] P. J. Lawreson, J. M. Stephenson, P. T. Blenkinsop, J. Corda, and N. N. Fulton, "Variable-speed switched reluctance motors," *IEE Proc. B*, vol. 127, no. 4, pp. 253–265, Jul. 1980, doi: [10.1049/ip-b.1980.0034](https://doi.org/10.1049/ip-b.1980.0034).
- [3] B. Jing, X. Dang, Z. Liu, and S. Long, "Torque ripple suppression of switched reluctance motor based on fuzzy indirect instant torque control," *IEEE Access*, vol. 10, pp. 75472–75481, 2022, doi: [10.1109/ACCESS.2022.3190082](https://doi.org/10.1109/ACCESS.2022.3190082).
- [4] R. Krishnan, *Switched Reluctance Motor Drives: Modeling, Simulation, Analysis, Design, and Applications*. Boca Raton, FL, USA: CRC Press, 2001.
- [5] S. E. M. Mohammadi, P. Chen, M. Moallem, B. Fahimi, and M. Kiani, "An alternate rotor geometry for switched reluctance machine with reduced torque ripple," *IEEE Trans. Energy Convers.*, vol. 38, no. 2, pp. 939–947, Jun. 2023, doi: [10.1109/TEC.2022.3229999](https://doi.org/10.1109/TEC.2022.3229999).
- [6] R. Reis, M. L. M. Kimpara, J. O. P. Pinto, and B. Fahimi, "Multi-physics simulations of 6/4 switched reluctance motor by finite element method," *J. Power Electron.*, vol. 26, pp. 9–18, Dec. 2020, doi: [10.18618/REP.2021.1.0004](https://doi.org/10.18618/REP.2021.1.0004).
- [7] J. Zhang, H. Wang, S. Zhu, and T. Lu, "Multi-physics multi-objective optimal design of bearingless switched reluctance motor based on finite-element method," *Energies*, vol. 12, no. 12, p. 2374, Jun. 2019, doi: [10.3390/en12122374](https://doi.org/10.3390/en12122374).
- [8] G. Fang, F. P. Scalcon, D. Xiao, R. P. Vieira, H. A. Gründling, and A. Emadi, "Advanced control of switched reluctance motors (SRMs): A review on current regulation, torque control and vibration suppression," *IEEE Open J. Ind. Electron. Soc.*, vol. 2, pp. 280–301, 2021, doi: [10.1109/OJIES.2021.3076807](https://doi.org/10.1109/OJIES.2021.3076807).
- [9] R. Abdel-Fadil, F. Al-Amyal, and L. Számel, "Torque ripples minimization strategies of switched reluctance motor—A review," in *Proc. Int. IEEE Conf. Workshop Óbuda Electr. Power Eng. (CANDO-EPE)*, Nov. 2019, pp. 41–46, doi: [10.1109/CANDO-EPE47959.2019.9110960](https://doi.org/10.1109/CANDO-EPE47959.2019.9110960).
- [10] X. Sun, J. Wu, G. Lei, Y. Guo, and J. Zhu, "Torque ripple reduction of SRM drive using improved direct torque control with sliding mode controller and observer," *IEEE Trans. Ind. Electron.*, vol. 68, no. 10, pp. 9334–9345, Oct. 2021, doi: [10.1109/TIE.2020.3020026](https://doi.org/10.1109/TIE.2020.3020026).
- [11] F. P. Scalcon, T. S. Gabbi, R. P. Vieira, and H. A. Gründling, "Performance improvement of switched reluctance motors via particle swarm algorithm," *J. Power Electron.*, vol. 25, no. 4, pp. 492–502, Dec. 2020, doi: [10.18618/REP.2020.4.0038](https://doi.org/10.18618/REP.2020.4.0038).
- [12] N. Saha, S. Panda, and D. K. Sahoo, "Modified whale optimization technique for combined objective of torque ripple minimization & speed control of SRM drive," in *Proc. 3rd Int. Conf. Energy, Power Environ., Towards Clean Energy Technol.*, Mar. 2021, pp. 1–5, doi: [10.1109/ICEPE50861.2021.9404396](https://doi.org/10.1109/ICEPE50861.2021.9404396).
- [13] J. W. Jiang, B. Bilgin, B. Howey, and A. Emadi, "Design optimization of switched reluctance machine using genetic algorithm," in *Proc. IEEE Int. Electric Mach. Drives Conf. (IEMDC)*, Coeur d'Alene, ID, USA, May 2015, pp. 1671–1677, doi: [10.1109/IEMDC.2015.7409288](https://doi.org/10.1109/IEMDC.2015.7409288).
- [14] H. Li, B. Bilgin, and A. Emadi, "An improved torque sharing function for torque ripple reduction in switched reluctance machines," *IEEE Trans. Power Electron.*, vol. 34, no. 2, pp. 1635–1644, Feb. 2019, doi: [10.1109/TPEL.2018.2835773](https://doi.org/10.1109/TPEL.2018.2835773).
- [15] Z. Xia, B. Bilgin, S. Nalakath, and A. Emadi, "A new torque sharing function method for switched reluctance machines with lower current tracking error," *IEEE Trans. Ind. Electron.*, vol. 68, no. 11, pp. 10612–10622, Nov. 2021, doi: [10.1109/TIE.2020.3037987](https://doi.org/10.1109/TIE.2020.3037987).
- [16] A. Zahid and B. Bilgin, "Determining the control objectives of a switched reluctance machine for performance improvement in generating mode," *IEEE Open J. Ind. Appl.*, vol. 4, pp. 99–110, 2023, doi: [10.1109/OJIA.2023.3256364](https://doi.org/10.1109/OJIA.2023.3256364).
- [17] M. Moallem, "Performance characteristics of switched reluctance motor drive," Ph.D. dissertation, Dept. Elect. Eng., Purdue Univ., West Lafayette, IN, USA, 1989.
- [18] B. Bilgin, J. W. Jiang, and A. Emadi, *Switched Reluctance Motor Drives: Fundamentals to Applications*. Boca Raton, FL, USA: CRC Press, 2019.
- [19] R. Sashankh, "Multi-objective optimization of the switched reluctance motor for improved performance in a heavy hybrid electric vehicle application," M.S. thesis, Dept. Elect. Eng., Purdue Univ., West Lafayette, IN, USA, 2016.

- [20] A. Chithrabhanu and K. Vasudevan, "Quantification of noise benefits in torque control strategies of SRM drives," *IEEE Trans. Energy Convers.*, vol. 38, no. 1, pp. 585–598, Mar. 2023, doi: [10.1109/TEC.2022.3201325](https://doi.org/10.1109/TEC.2022.3201325).
- [21] P. Pillay and W. Cai, "An investigation into vibration in switched reluctance motors," *IEEE Trans. Ind. Appl.*, vol. 35, no. 3, pp. 589–596, May/Jun. 1999, doi: [10.1109/28.767007](https://doi.org/10.1109/28.767007).



RENATA REZENDE C. REIS was born in Campo Grande, Brazil, in 1993. She received the B.S. and M.S. degrees in electrical engineering from the Federal University of Mato Grosso do Sul, Campo Grande, in 2019 and 2022, respectively. Her research interests include power electronics, electric machines design and drives, and electrical power systems.



MARCIO L. MAGRI KIMPÁRA (Member, IEEE) was born in Jales, Brazil. He received the B.S. and M.S. degrees in electrical engineering from the Federal University of Mato Grosso do Sul, Campo Grande, Brazil, in 2009 and 2012, respectively, and the Ph.D. degree from the Federal University of Itajuba (UNIFEI), Brazil, in 2018. He has been a Faculty Member (On leave) with the Federal University of Mato Grosso do Sul, since 2022. He is currently a Postdoctoral Research with the

Oak Ridge National Laboratory, Oak Ridge, TN, USA.



LUIGI GALOTTO JR. (Member, IEEE) received the bachelor's degree in electrical engineering from the Federal University of Mato Grosso do Sul (UFMS), Campo Grande, Brazil, in 2003, the master's degree in artificial intelligence applications with the study of sensor fault-tolerant operation in drive systems, in 2006, and the Ph.D. degree in power electronics from Paulista State University, Ilha Solteira, Brazil, in 2011. Since 2013, he has been an Adjunct Professor and a Researcher with the UFMS. He has been involved in several development projects, including, sensor monitoring and diagnosis, spectrum analyzers, sensors fault-tolerant operation methodology, and converters for photovoltaic generation. His research interests include power electronics, control systems, and applied artificial intelligence and statistics techniques.



JOÃO ONOFRE PEREIRA PINTO (Senior Member, IEEE) was born in Valparaíso, Brazil. He received the B.S. degree in electrical engineering from Universidade Estadual Paulista, Brazil, in 1990, the M.S. degree from Universidade Federal de Uberlândia, Brazil, in 1993, and the Ph.D. degree from The University of Tennessee, Knoxville, TN, USA, in 2001. He was a Faculty Member of the Federal University of Mato Grosso do Sul (UFMS), Campo Grande, Brazil, from 1994 to 2021, where he was the Dean of the Engineering College, from 2013 to 2017. He was the Founder and the Director of BATLAB, artificial intelligence applications, power electronics and drives, and energy systems. He has been a Faculty Member (On leave) with the Federal University of Rio de Janeiro, Rio de Janeiro, Brazil, since 2021. He is currently a Senior Researcher with the Oak Ridge National Laboratory, Oak Ridge, TN, USA. He has more than 200 published papers in journals and conference proceedings. His research interests include power electronics, artificial intelligence applications, energy systems, and electrical machine drives.

...